

P2M.4 THE WRF MODEL AS A TOOL TO UNDERSTAND MESOSCALE PROCESSES ON THE POORLY SAMPLED SOUTH AMERICAN ALTIPLANO

José M. Gálvez¹, Raquel K. Orozco¹, and Michael W. Douglas²

¹ CIMMS/University of Oklahoma, Norman, OK 73069

² NSSL/NOAA, Norman, OK 73069

1. ABSTRACT

With the purpose of describing the mesoscale circulations and rainfall that occur over the South American Altiplano during the summer, and in particular the effects of the lakes and dry salt flats, temporary observing networks were deployed during the rainy season of 2002-2003, as part of the South American Low Level Jet Experiment (SALLJEX) activities. These included a 200-raingauge network in the vicinity of Lake Titicaca and two temporary ~ 6-station pilot balloon networks that operated during two short field experiments. Even though the data collected were useful to describe certain features of the mesoscale circulations and rainfall, the lack of additional observations in and around the region, added to the Altiplano's complex terrain, produced many gaps on the description of the atmospheric processes, which could only be filled with the aid of numerical simulations using a mesoscale model.

The Weather Research and Forecasting (WRF) model was chosen based on computer capabilities, ample documentation and support, model flexibility, and future trends. The main goal with the numerical simulations was to describe the nocturnal lake-effect storms that occur over Lake Titicaca and associated mesoscale processes such as the advection of moisture into the Altiplano through the eastern canyons and overall terrain-induced circulations related to the diurnal cycle.

Several test simulations were initially carried out using different domains and resolutions. The final (FNL) analyses from the Aviation Model (AVN) were utilized as initial and boundary conditions. Initially, the WRF model proved to resolve – in certain regions - the late afternoon maximum of convection over the Altiplano associated to the diurnal cycle with a horizontal resolution of 10 km and 31 sigma levels in the vertical. The convective parameterization scheme utilized was the Kain-Fritsch scheme and the Lin et. al. for the microphysics. The nocturnal convection over Lake Titicaca was, however, not present in these simulations. An error on the specification of the surface temperature of the lake was identified and corrected by setting it to a constant value of 13°C. Further test simulations indicated that a resolution of 1 km at the most was necessary to reproduce the lake breezes and therefore the nocturnal lake-effect storms induced by Lake Titicaca.

These and additional results as well as comparisons with observations will be presented on a poster. The implications of the use of a mesoscale numerical model such as the WRF to simulate the mesoclimate in poorly sampled regions will be discussed as well. An extended version of the present study can be found at: <http://www.nssl.noaa.gov/projects/pacs/web/ALTIPLANO/NF/>.

2. HISTORY AND MOTIVATION

The South American Altiplano is an elevated plateau (~ 3700 m ASL) and also a closed basin located in the Central Andes between 14°S and 22°S. The geographical

* Corresponding author address: José M. Gálvez
CIMMS/OU, 1313 Halley Circle, Norman OK,
73069. Email: jose.galvez@noaa.gov

bounds are the Amazon Rainforest to the east and northeast, the Chaco to the southeast and by the Atacama Desert to the west. Many lakes and dry salt flats (so called "salares") shape the landscape. The two largest are Lake Titicaca and Salar de Uyuni. Even though the Altiplano has been studied the large scale, no previous study has described with detail the mesoclimate of the region, in particular the roles of the lakes and dry salt flats in the modulation of rainfall.

Nocturnal convection was initially observed over Lake Titicaca through rainfall climatologies and satellite imagery. Figure 1 shows the mean annual rainfall accumulated between 1957 and 1961. The analysis shows a maximum over the lake of more than $1100 \text{ mm year}^{-1}$ contrasting with less than 800 mm year^{-1} around it. Another climatological rainfall analysis obtained from the bi-national Peruvian-Bolivian Lake Titicaca Commission suggested an even stronger maximum of $1400 \text{ mm year}^{-1}$.

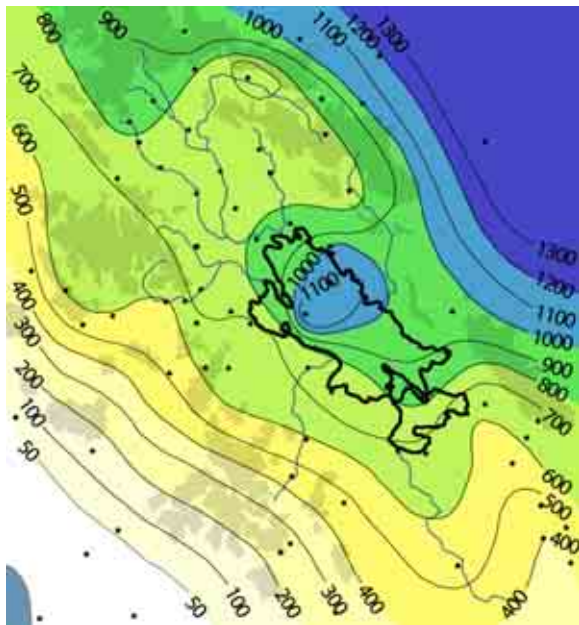


Figure 1. Mean Annual Rainfall in the Lake Titicaca (mm year^{-1}) area accumulated from 1957 to 1961. This figure was extracted from Kessler and Montheim (1968) after Schwerdtfeger (1976) and reformatted.

As part of the Panamerican Climate Studies Sounding Network (PACS-SONET)

activities, a workshop and short field experiment were programmed in Bolivia during December 2000. The main goal was to spin up the meteorological activities in this country to support the pilot balloon network established in 1999. The second objective was to make people appreciate pilot balloon data so they could use the PACS-SONET database, in particular the observations made in Bolivia.

The workshop was held in La Paz but the 3-day field campaign was carried out in the shores of Lake Titicaca to explore the breezes and their possible relation to nocturnal storms over the lake. The sampling period coincided with a quite active lake effect storms period, which served as additional motivation for a further deeper study. Figure 2, taken during the PACS-SONET December 2000 field experiment, shows a nocturnal lake effect convective storm that developed near the western shore of Lake Titicaca.

The South American Low Level Jet Experiment (SALLJEX) was programmed for the rainy season of 2002 and 2003 starting in November and ending in February. The SALLJEX had a series of funded projects, 3 of which were organized by the NSSL but none of these focused on the Altiplano meteorology, since the main goal of the SALLJEX was to describe the moisture flux from the tropics into the subtropics that occurs over a north-south corridor in the lowlands east of the Andes.

The SALLJEX, however, represented a great opportunity to sample the Altiplano given the large number of observations programmed. Furthermore, numerous South American individuals with an interest in weather and climate were available for field studies. On the other hand, the budgets available for Altiplano activities were reduced. Taking these 3 facts into account several activities were organized to sample the Altiplano during the rainy season of 2002-2003 using inexpensive technology but maximum participation.



Figure 2. Nocturnal lake effect storm that developed to the west of Lake Titicaca during the 3-day long Lake Titicaca Experiment in December 2000.

The Altiplano observing networks consisted on a simple 200-station raingauge network and two short field experiments based mainly on 5 to 7 pilot balloon station networks that were operated during periods from 5 to 7 days. The networks are presented in figure 3. The data obtained through these networks were sufficient to:

- 1) Describe the diurnal variability of the horizontal and vertical motion fields near Lake Titicaca and Salar de Uyuni during the warm season.
- 2) Measure the diurnal variations of certain surface properties such as temperature and wind during the same period of time.
- 3) Map the precipitation fields during the warm season with higher spatial density over the Lake Titicaca region and relate them to the motion fields.
- 4) Describe the diurnal variations of cloudiness and relate them to the motion and rainfall fields.
- 5) Compare satellite-estimated cloudiness fields with rainfall measurements.

Some limitations of the data sets due to either problems in the logistics or the reduced budget included the lack of

moisture soundings and the lack of data in certain regions of the Altiplano that were key for the understanding of the atmospheric processes involved in the modulation of rainfall. Considering these limitations a short modeling study was carried out to better describe these processes through numerical simulations. An emphasis in the circulations induced by Lake Titicaca was applied. The study is still being developed but some preliminary results are presented in this manuscript.

5. MODELING STUDY

The numerical simulations performed using the Weather Research and Forecasting (WRF) Model served as a key tool to understand what may be occurring in the region during lake-effect storm events.

The WRF Model is a next-generation numerical model designed for weather prediction purposes with a major focus on the simulation of mesoscale processes. It is the result of a multi institutional effort as it has been developed by the Mesoscale and Microscale Meteorology Division of the National Center of Atmospheric Research (NCAR/MMM), the National Centers for Environmental Prediction (NOAA/NCEP), the Forecast Systems Laboratory (NOAA/FSL), the University of Oklahoma Center for the Analysis and Prediction of Storms (CAPS) and the U.S. Air Force Weather Agency (AFWA).

The design of the WRF started in 1998, targeted for the 1-10 km grid-scale and intended for operational weather forecasting, regional climate prediction, air-quality simulation, and idealized dynamical studies, with the idea of eventually replacing the existing mesoscale numerical models such as the MM5, ETA and RUC.

The WRF initial design allowed for multiple dynamical cores, one based on height coordinates, and one based on mass coordinates. The horizontal staggering was

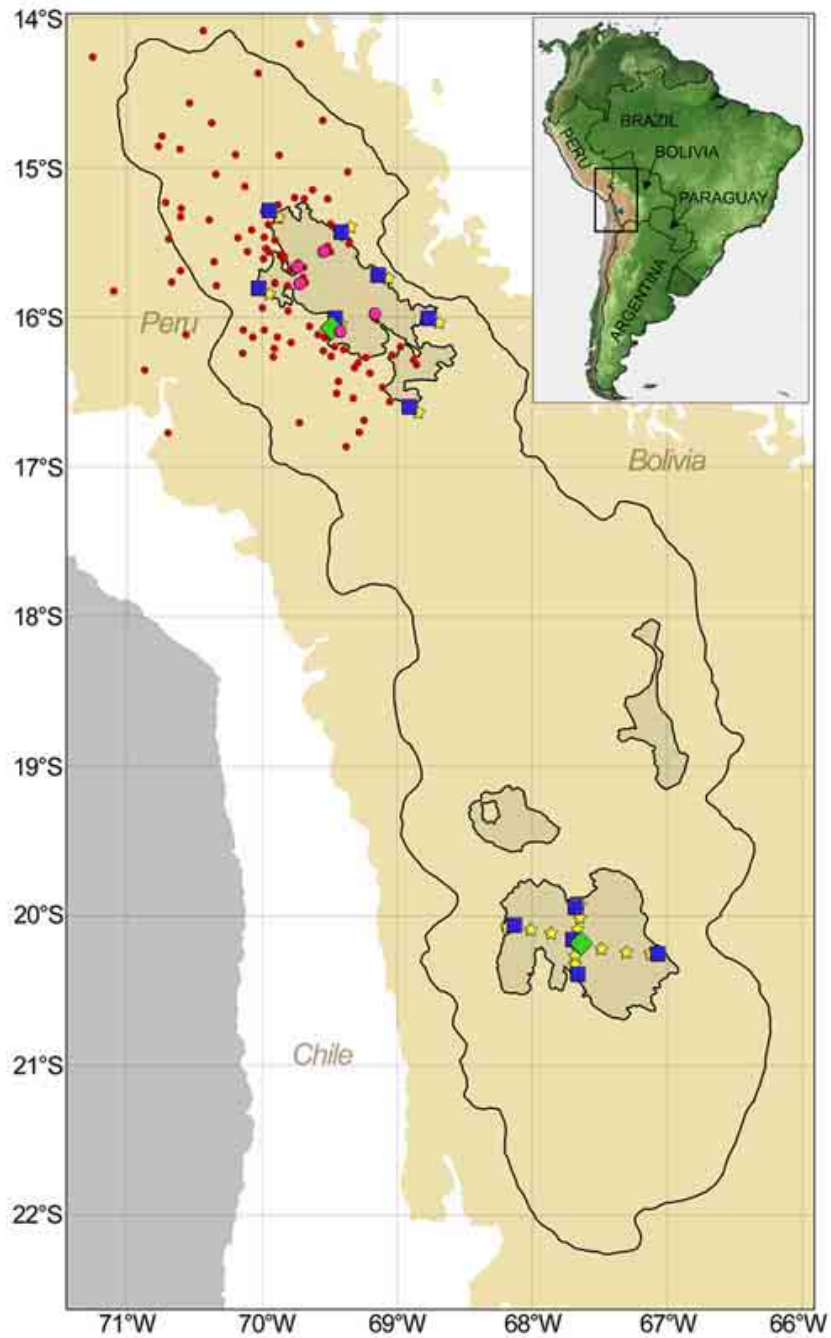


Figure 3. Enhanced networks that operated in the Altiplano during the SALLJEX. The Altiplano basin is indicated with a solid black line. From north to south, Lake Titicaca, Lake Poopó, Salar de Coipasa and Salar de Uyuni are indicated with solid black lines and shaded in gray. The terrain higher than 3000 m ASL is shaded in light brown. The 98-data point raingauge network available after quality control procedures is indicated with small red dots. The five digital raingauges installed in Lake Titicaca are indicated with large pink circles. The pilot balloon stations operated during the Titicaca and Uyuni Experiments are indicated with blue squares. The tetheredsonde and radiosonde stations are indicated with green diamonds. The yellow stars indicate temperature measurements.

the Arakawa C-grid. The large time steps utilized a third-order Runge-Kutta scheme, and second to sixth order advection operators could be chosen to solve the advection equation. The main effort when developing the WRF Model was improving the numerics.

The FNL analyses from the Aviation Model (AVN) were utilized as initial and boundary conditions. They are analysis created later than the operational analyses, therefore they take into account a larger number of observations and are closer to reality.

These analyses have a horizontal resolution of 1 degree and 24 pressure levels in the vertical. The variables contained are surface pressure, sea level pressure, geopotential height, temperature, relative humidity, zonal wind, meridional wind, vertical velocity, vorticity, sea surface temperature, ice cover and ozone content.

In order to explicitly simulate the lake-effect convective storms, a fine horizontal resolution not larger than 1 km was necessary. At this resolution the model was able to reproduce the land-lake nocturnal breezes and the lines of low-level convergence that form over the lake and lead to the convective storms.

Based on the numerical simulations and on analyses put together using satellite images the nocturnal lake-effect storms seem to be sensitive not only to the amount of moisture available in the Altiplano boundary layer but to the moisture advected through the canyon located to the east-northeast of the Lake. This connection could not be established only from the pilot balloon, surface and rainfall observations, which implies the applicability of the simulations and satellite data as additional tools to study the atmosphere in regions with poor observing networks.

The experimental design included three 1-domain 1.3-km horizontal resolution

simulations for lake-effect storm days, two 1-km horizontal resolution runs for two days with different synoptic wind scenarios and finally one 2-domain nested run for a lake-effect storm day, with a horizontal resolution of 5km for the outer domain and 1km for the inner one. Results from the two latest experiments are presented in this document. Results from the three will be included in the poster.

4. VALIDATION PRODUCTS

The observations from the Altiplano campaigns as well as GOES-8 infrared satellite imagery composites were utilized for validation.

The results from the raingauge network confirmed that the largest rainfall totals occur in the islands to the northeast of Lake Titicaca extending to the northeastern shore of the lake. This area of high rainfall can be associated to nocturnal low-level convergence since lake-induced divergence and associated cloud free skies dominate the region during most of the day. The rainfall field over the central lake and eastern shore, however, was not resolved due to the lack of islands and the lack of data in the Bolivian side.

An analysis sketched using a selection of 30 days in which lake-effect-storms developed was constructed and displayed in figure 4. Even though no observations were obtained near the lake SE-NW axis given the reduced number of islands, it shows the presence of a region of high rainfall over the lake, with the maximum located towards the eastern islands and shore. In Isla Soto the averaged daily rainfall exceeded 12 mm day^{-1} which corresponds to $\sim 0.5 \text{ inch day}^{-1}$. This almost doubled the amount of rainfall collected over land, and tripled the amount of rainfall collected in the region located to the southwest of the lake. The latter, however, is also affected by the northeast-southwest Altiplano rainfall gradient associated to the distribution of low-level moisture by the

atmospheric circulation. The region of the largest rainfall is located in the northeastern Altiplano because during the rainy season the region is exposed to periods of mid-tropospheric easterly flow which lead to moisture flux from the Amazon Basin through the eastern slopes of the Andes favoring the development of moist convection. To the

south the periods of easterly flow are reduced and, in contrast, westerly flow favors the advection of very dry air from the Pacific. Closeness to the moisture source is also a factor that regulates rainfall in the Altiplano, which explains the east-west component of the gradient.

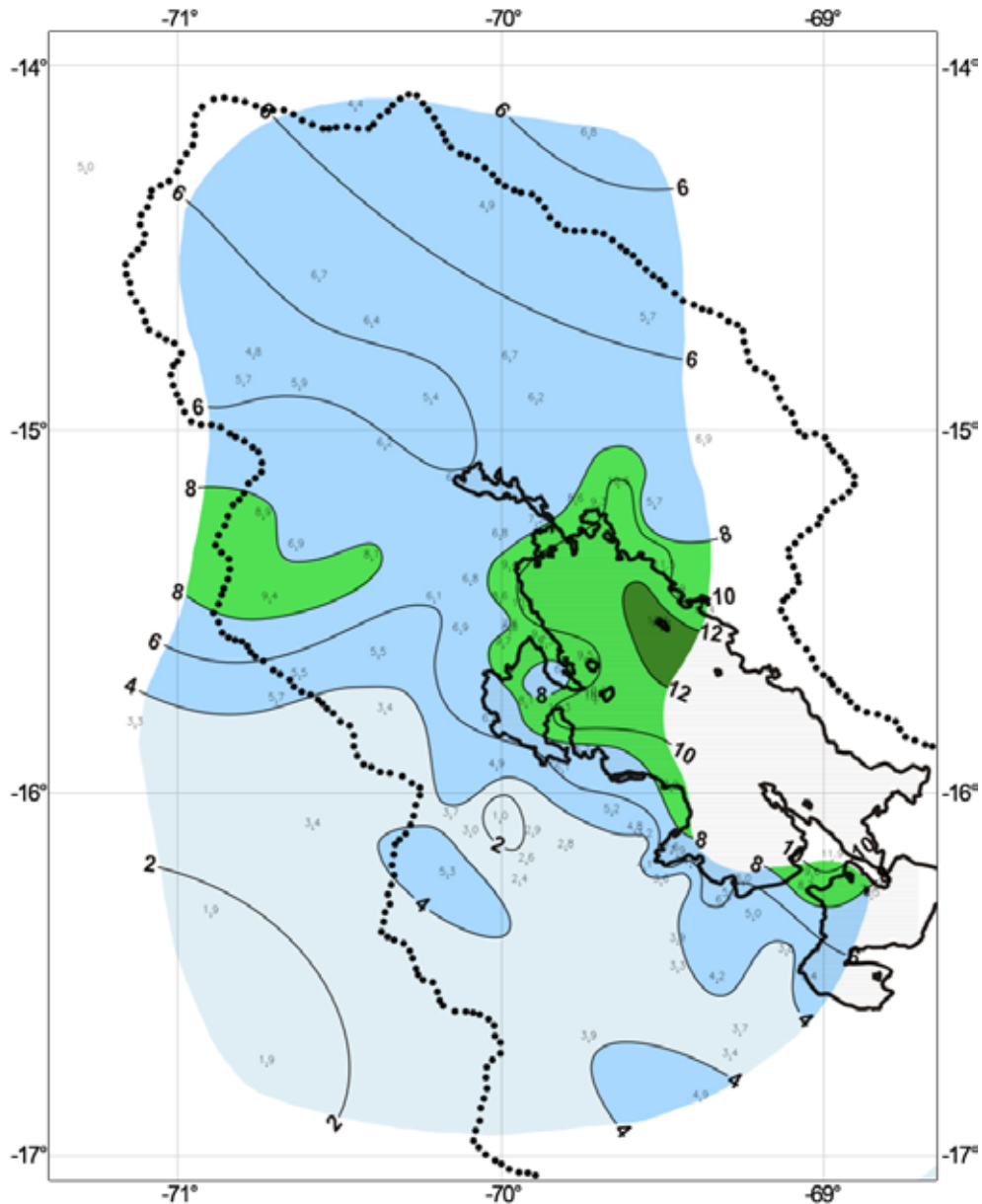


Figure 4. Daily rainfall averaged over 30 selected lake-effect-storm days. Lake Titicaca is indicated with a thick black line. The Altiplano basin is indicated with a thick dotted line. The rainfall is contoured every 2 mm and shaded every 4 mm.

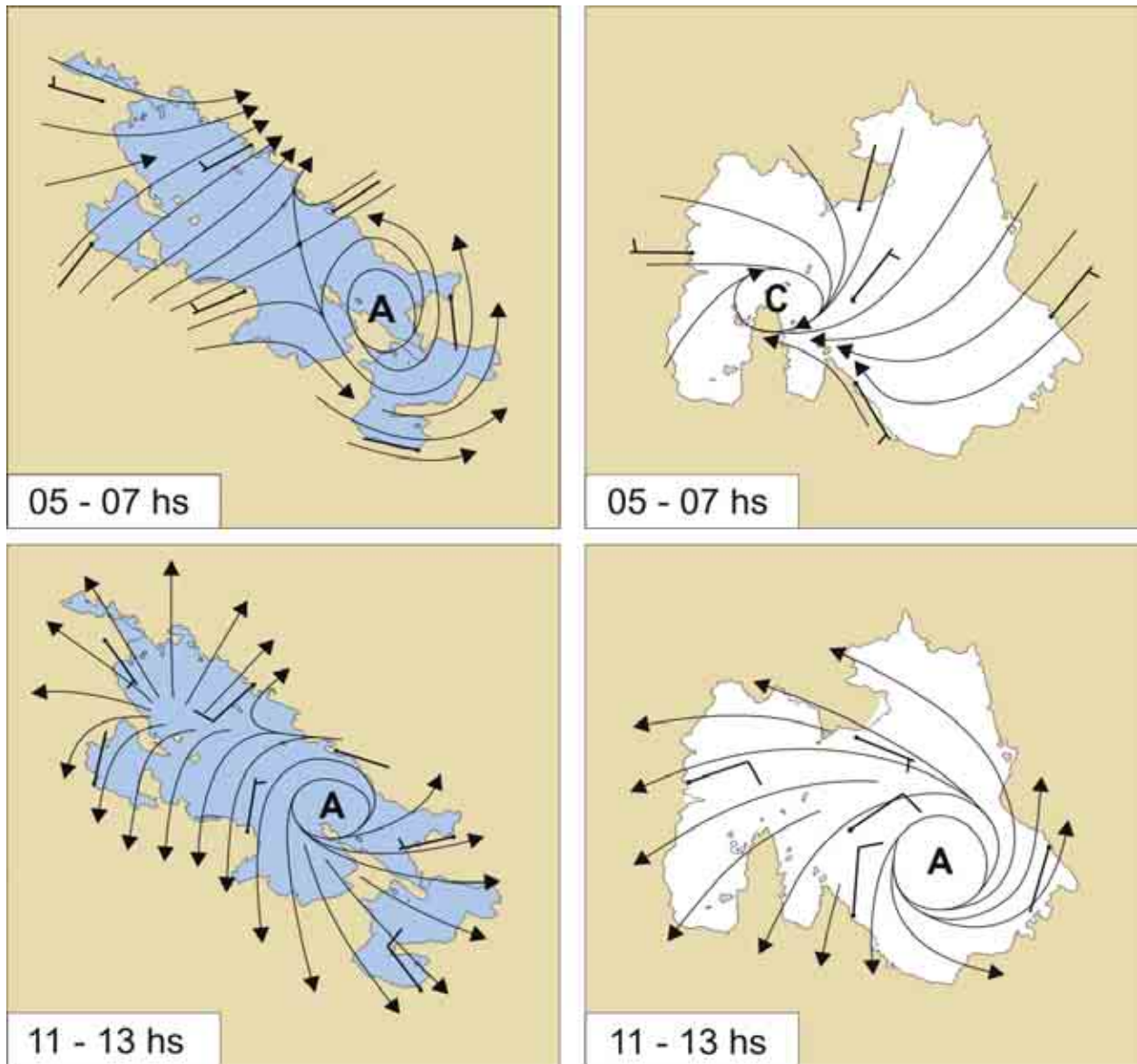


Figure 5. Breeze signal at 150 m AGL over Lake Titicaca (left) and Salar de Uyuni (right). The top and bottom panels correspond to the morning (05-07 LST) and near noon (11-13 LST) characteristic circulations. The mean wind profiles were removed for each station to extract the synoptic flow and obtain a clean breeze signature.

The pilot balloon observations were utilized to calculate the breeze signal for morning and afternoon hours (figure 5). After the observations were cleaned and transformed into wind data, the daily winds averaged over each station were calculated and subtracted from each station for each hour. The purpose was to remove the synoptic flow and obtain a clear signature of the breezes, which can be depicted as an anomaly from the mean flow. The results were organized in 3-hour periods and the periods

between 05 and 07 LST are plotted for Lake Titicaca (left panels) and Salar de Uyuni (right panel). The Lake Titicaca breeze signal was quite disorganized during the morning but a region of confluence was evident over the central part of the lake. During the afternoon the diffluent nature of the flow was evident from the observations with breezes as strong as 10 knots in two of the stations (Guaqui to the south and Conima to the northeast).

Divergence was calculated using polygons sketched with the pilot balloon stations. The method utilized is described by Davies-Jones (1993) and consists on fitting a linear windfield to the observations in order to calculate the divergence and vorticity. Unfortunately, the lack of nocturnal observations in all the sites at the same time as a result of the strong winds limited the calculations of divergence during between 20 LST and 06 LST.

The results (figure 6) show the hourly divergence at 150 m AGL averaged over the 5-day period. They show divergent flow over both the lake and the salar during the day, with stronger divergence over the salar. The few observations gathered during nighttime suggest that the convergence over the lake was stronger than the one over the salar. A counterintuitive result is that the period of maximum convergence occurs during the evening instead of the early morning, as expected. This period of large low-level convergence can be associated to the collision between easterly flow that originates in the eastern slopes of the Andes and westerly flow that originates in the western slopes, according to results from the pilot

balloons, satellite images and numerical simulations. Whenever moisture in the Altiplano is sufficient, moist convection develops when this region of convergence propagates over the highly-buoyant Lake Titicaca low-level atmosphere. Furthermore, when storms develop in the western mountain range and propagate towards the lake, they intensify whenever they migrate over the lake region as well.

As a final validation product, GOES-8 infrared CH₄ satellite images were used to construct the diurnal cycle of convection for the Lake Titicaca region. Figure 7 shows the frequency of clouds colder than -15°C for different times of the day. This threshold was utilized since leads to the highest correlations between rainfall and radiance in station located close to the lake. Even though the largest frequency of cold clouds can be observed in the western Altiplano during the late afternoon, the clouds that form or propagate over the lake produce larger rainfall rates. A moister environment over the lake than over land, as suggested by numerical simulations, appears to be the reason. Notice, however, the clear presence of cold clouds over the lake during the night.

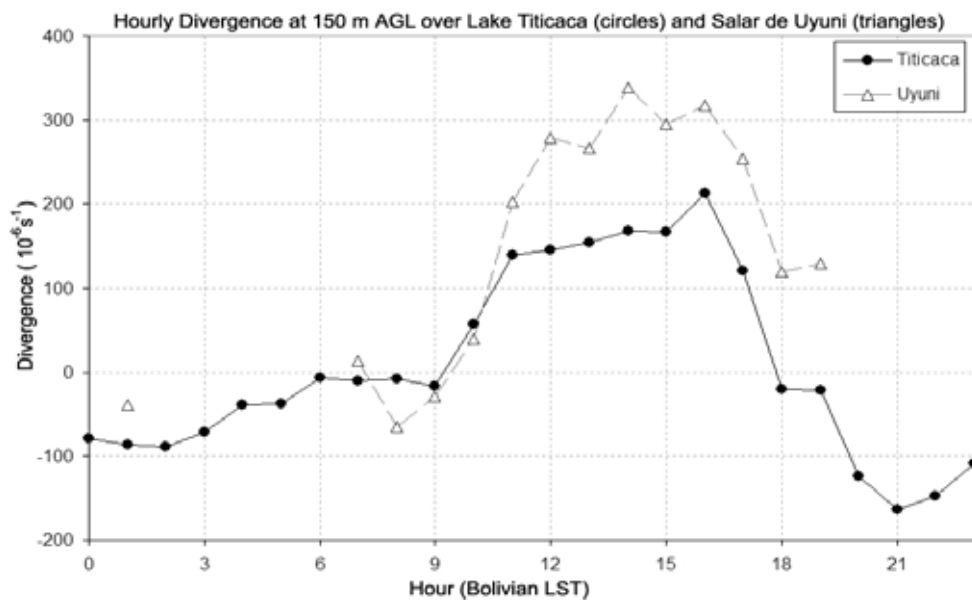


Figure 6. Diurnal cycle of horizontal divergence at 150 m AGL calculated over Lake Titicaca (circles) and the Salar de Uyuni (triangles). The calculations were made using polygons with the pilot balloon observations and assuming a homogeneous wind field (Davies-Jones, 1993).

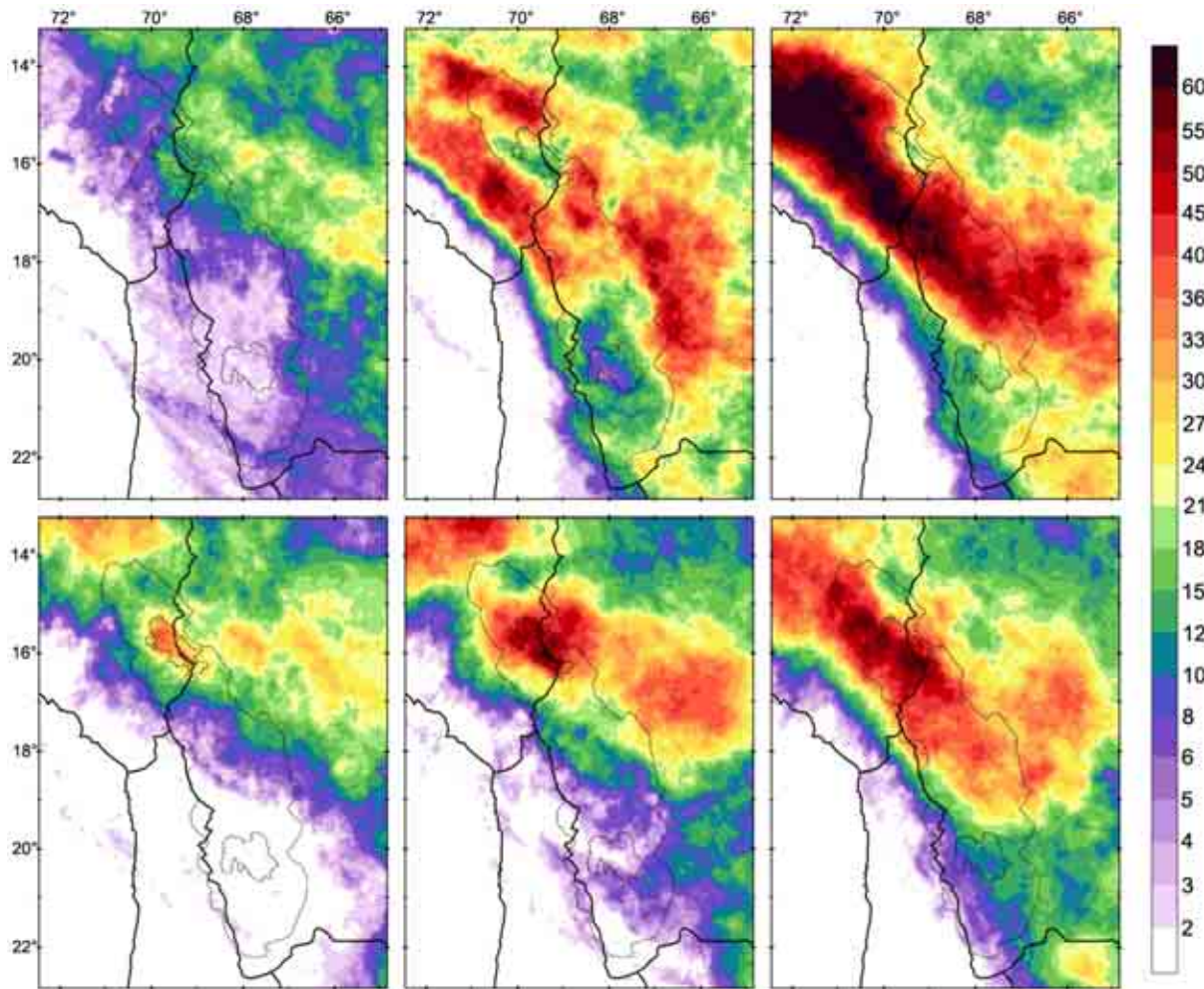


Figure 7. Frequency of clouds colder than -15°C calculated using 2002-2003 GOES-8 IR4 satellite images corresponding to 30 selected days in which lake-effect-storms developed. The selection was applied using the rainfall data. The upper-left panel corresponds to 8-12 LST, the upper-central to 12-16 LST, the upper-right to 16-20 LST, the lower-right to 20-00 LST, the lower-central to 00-04 LST and the lower left to 04-08 LST.

6. ANALYSIS AND RESULTS

The WRF model was successful in the description of the lake effect storms and associated circulations that develop over Lake Titicaca. To achieve simulations that were considered representative, however, the model had to be tuned by adjusting some surface properties. The lake surface temperature was found to be set to 0°C , which initially lead to a total absence of nocturnal convection. After this problem was discovered the temperature was set to the climatological value of 13°C (Carmouze, 1991). Additional trial simulations revealed that the storms were better reproduced when

using a horizontal resolution of 1km. For simulations with resolutions finer than 5km the convective parameterizations were turned off for the model to simulate the convection explicitly.

The lake-induced breezes and nocturnal convection were successfully simulated by the WRF Model. Figure 9 shows the results obtained in the 1-km horizontal resolution inner domain from the 2-domain nested simulation. The structure of the circulations and associated convection, however, was better simulated during the night than during the day in due to a problem with the land-surface temperature. According

to the model the surface temperature west of Lake Titicaca remained below 20°C during the entire simulation period, and in flat areas or valleys away from the lake the surface temperature did not exceed 16°C (figure 8, second panel). These unusually low temperatures affected the development of the convection over land in two ways. (1) Low values of low-level buoyancy were not sufficient to trigger the afternoon convection, and (2) the weak lake-land temperature gradient did not allow the generation of a strong lake breeze reducing as well the magnitude of the low-level convergence over the western Altiplano. Even though low-level moisture appeared to be sufficient to lead to afternoon moist convection in the region (Garreaud, 1998), this was constrained to areas in which the land temperature exceeded 20°C and appeared isolated and short lived (figure 9 between 12 and 20 LST to the west of the lake). The inaccuracies were observed in response to errors in the 1° base skin temperature climatological input file and have not been tuned yet.

The model was successful, however, in simulating the afternoon convection over the eastern slopes and eastern mountain range as well as convection over the Altiplano located to the southeast of the lake. In the latter the land-surface temperatures were high (skin temperature > 20°C during the morning and afternoon as suggested by figure 8) and the low-level buoyancy was sufficient to trigger storms during the afternoon with the aid of low-level convergence of terrain-induced breezes.

According to the model, the maximum intensity of the lake breezes that developed was of 1 to 7 m s⁻¹ near 16 LST, but they did not penetrate far away into the land. During the night, the magnitude of the breezes near the coast was of about 3 to 6 m

s⁻¹ but over the lake the breezes exceeded 7 m s⁻¹ in several locations. The flow clearly accelerated over the water in response to a smaller roughness length. Lines of convergence formed in different locations but the main one formed and remained east of the lake axis in response to a stronger breeze from the western shore of the lake. This breeze was stronger in response to a larger temperature gradient between the western land and the coast when compared to the one in the eastern shore. The same pattern was observed in several simulations (not presented in this manuscript), which suggest this process as the reason why the largest rainfall rates are found east of the NW-SE lake axis.

Even though the storms that occur west of the lake and propagate over it during the evening were not simulated, a group of storms originated over land to the southeast of the lake in the nested simulation's inner domain and propagated towards the lake region by 22 LST. After reaching the lake region the storms intensified. To study the evolution of these storms selected timeseries from three 9-gridpoint sectors were analyzed. The storm triggered to the southeast of Lake Titicaca, over terrain that divides the lake basin and the La Paz canyon during the late afternoon and propagated towards the lake during the evening. Redevelopment and strengthening was observed when the system moved over the lake as satellite imagery suggested when storms from the west propagated over the lake. Figures 11 and 12 show the potential temperature, and equivalent potential temperature fields during the simulation period. Even though the vertical velocity field could not be presented, the updraft velocities are larger over the lake than over the terrain around it.

10 mAGL wind in m s^{-1} (colored streamlines) and rainfall in mm (contour)

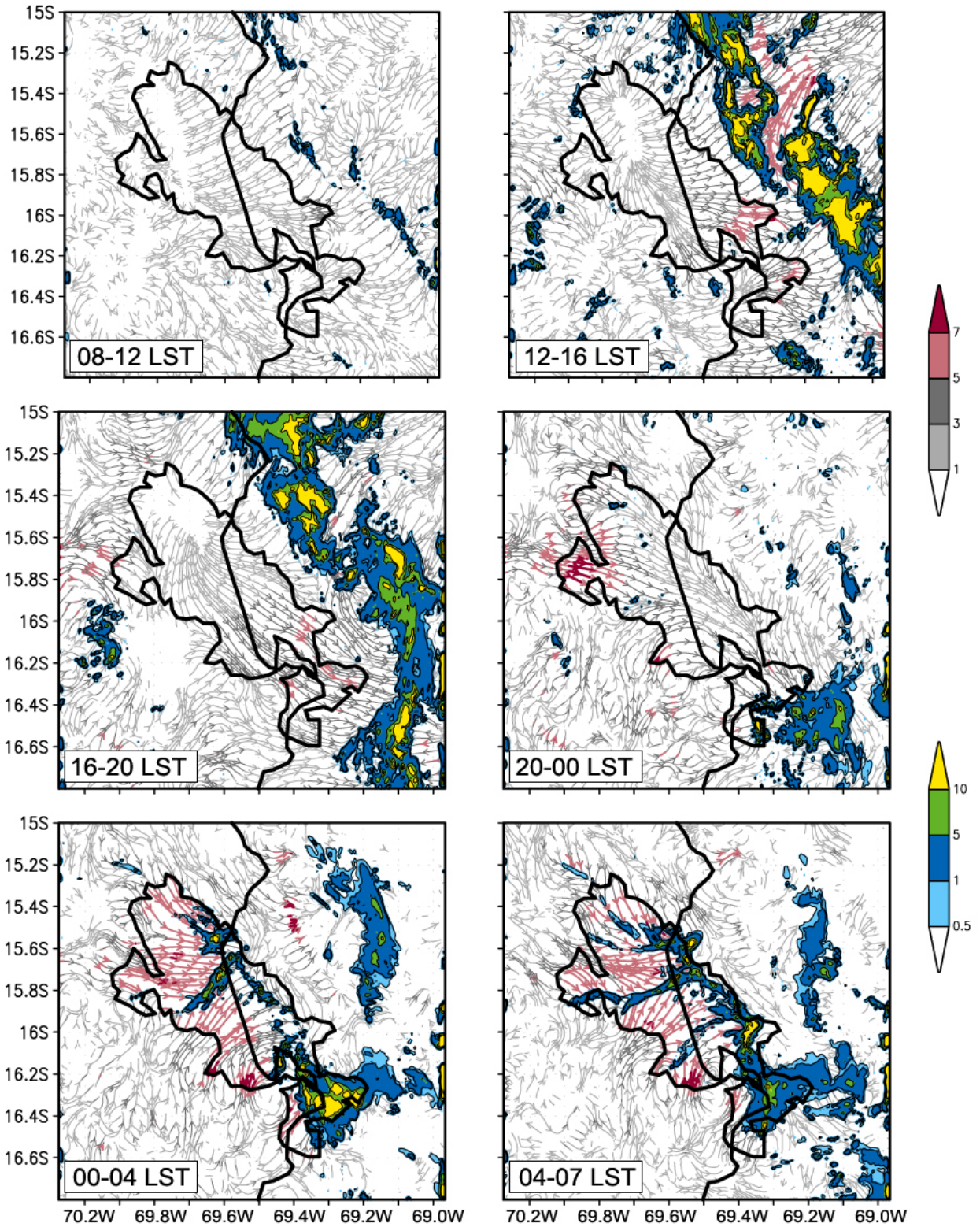


Figure 8. Rainfall and 2 mAGL winds averaged during 4-hour intervals throughout the 1-km nested simulation.

Specific humidity at 2m (shaded) and vertical velocity at 550 mb in m s^{-1} (contour)

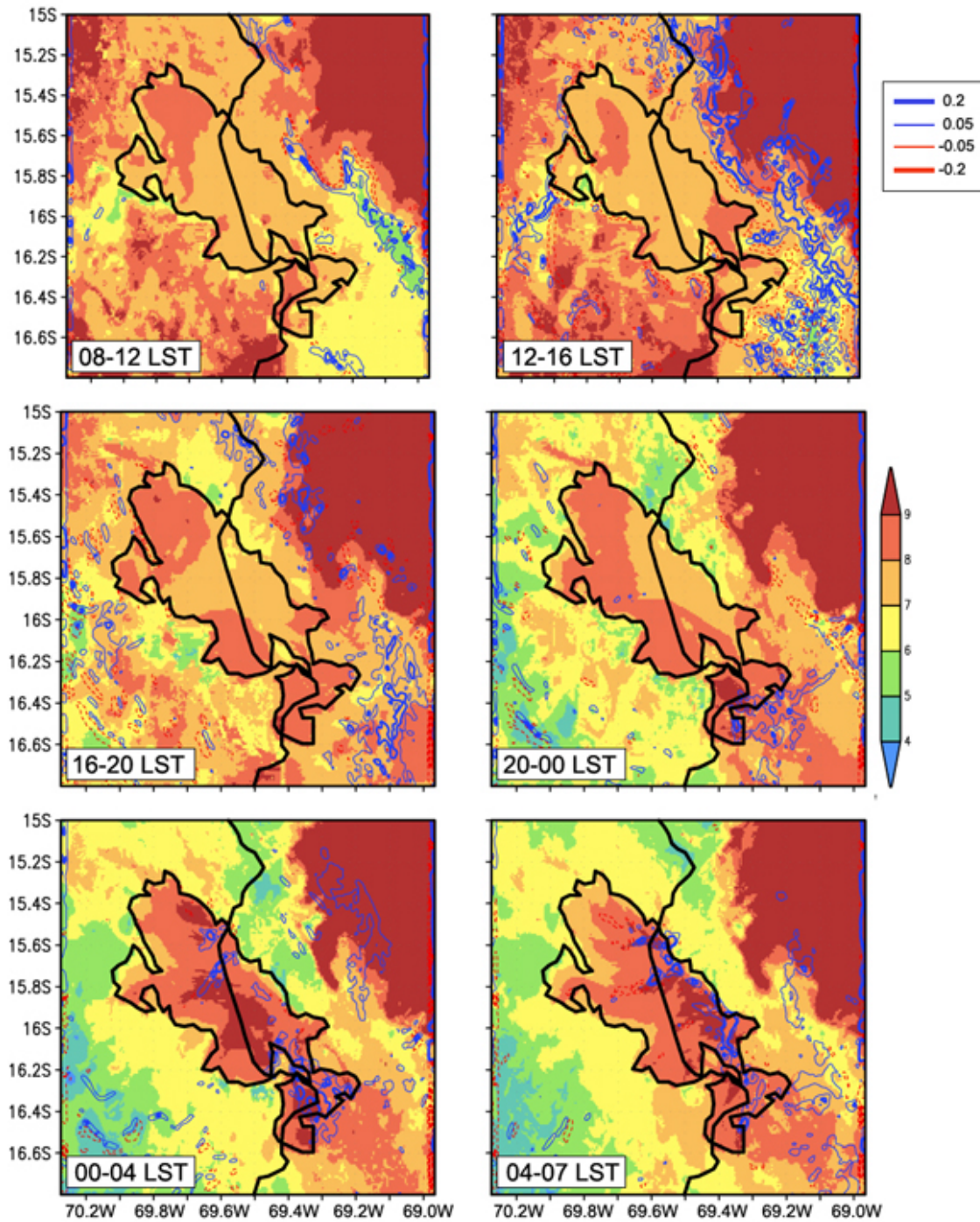


Figure 9. Specific humidity at 2 mAGL and vertical velocity at 550 mb averaged during 4-hour intervals throughout the 1-km nested simulation.

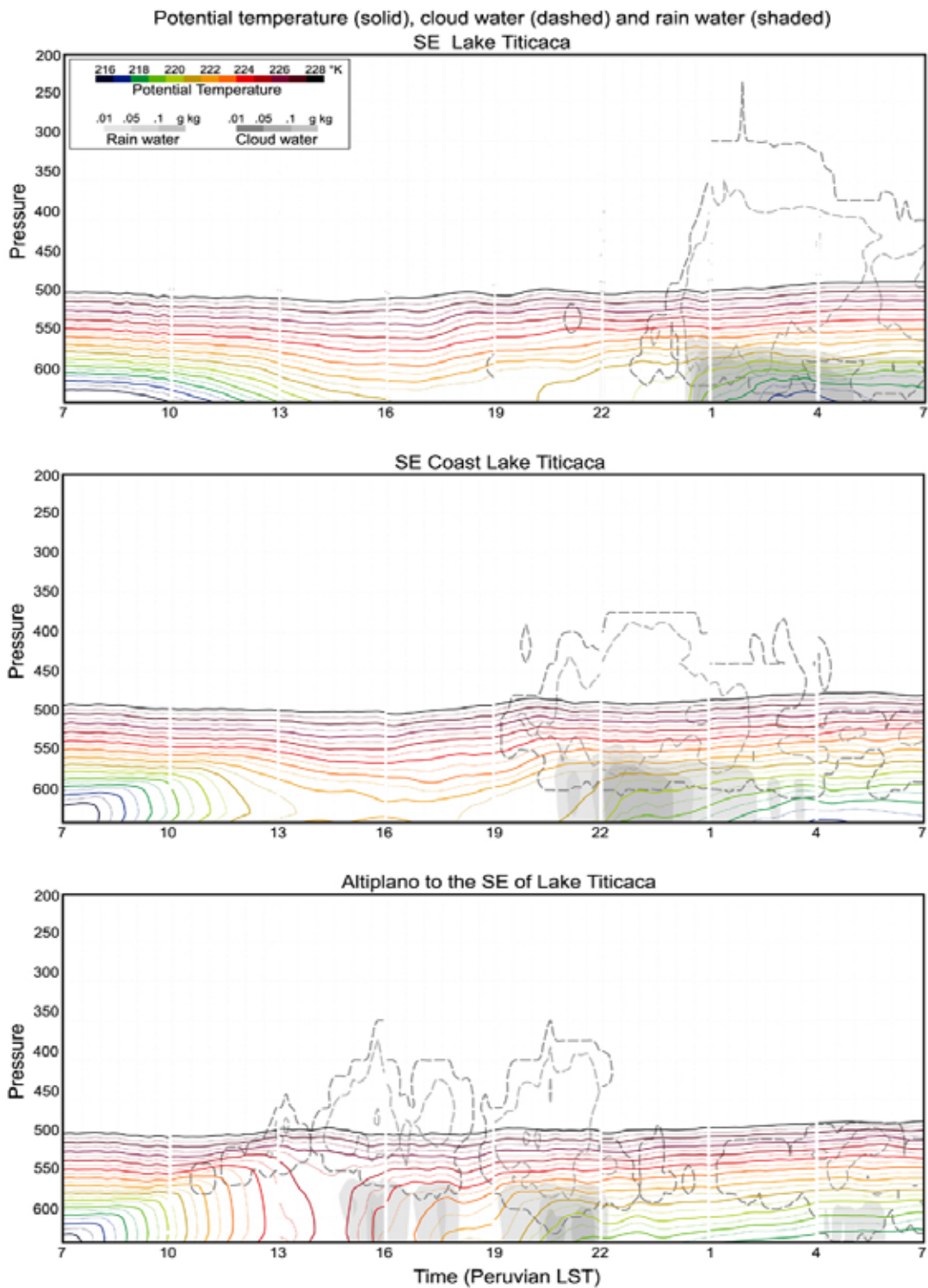


Figure 10. Timeseries of potential temperature (colored solid contours), cloud water (dashed contours) and rain water (shaded) averaged over 9 grid points at three locations in the southeastern end of the lake (upper panel), the southeastern coast (middle panel) and the Altiplano southeast of the lake. The timeseries start at $t=00$ (25 January 2003 at 7 am Peruvian LST) and end at $t=24$ (26 January 2003 at 7am Peruvian LST).

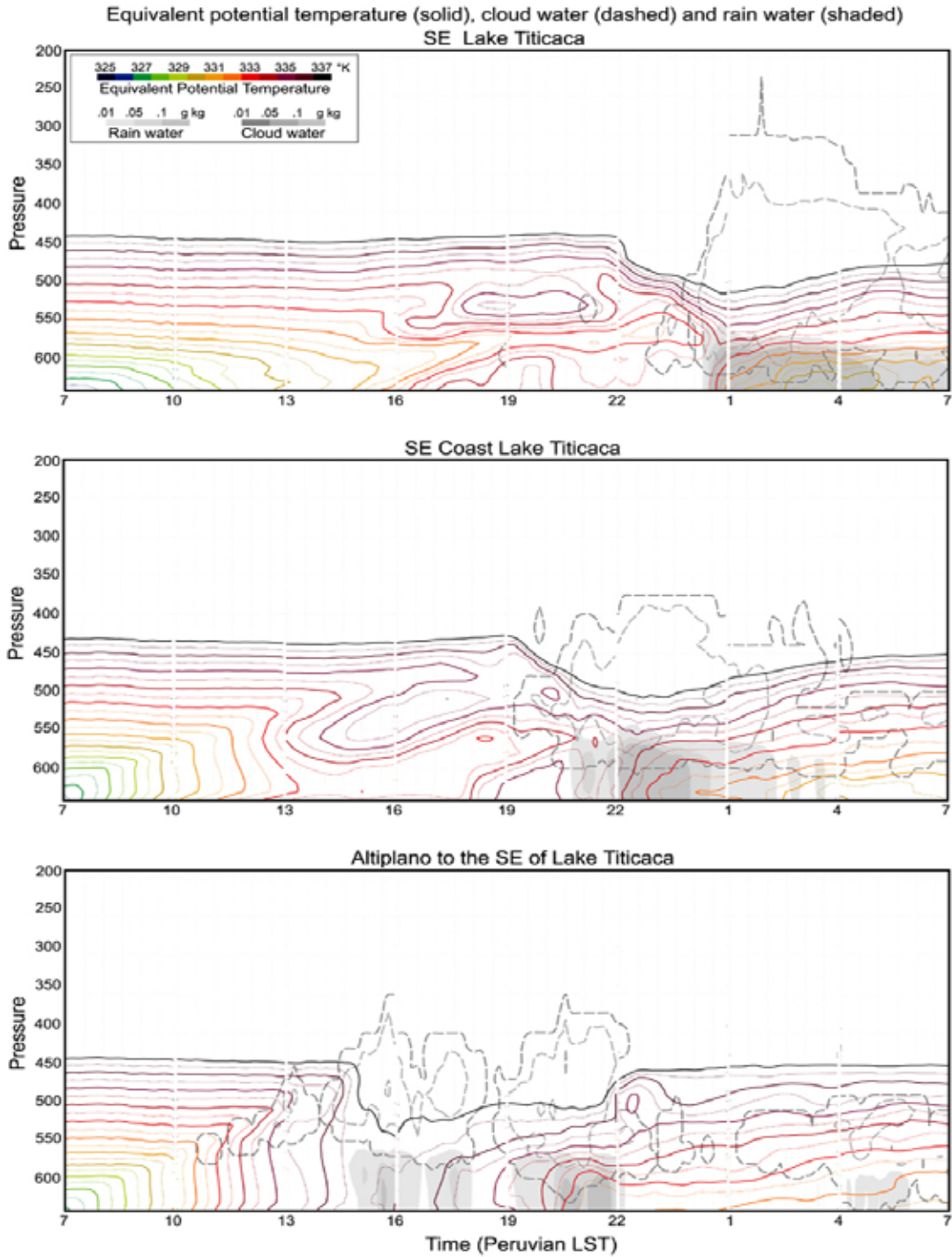


Figure 11. Timeseries of equivalent potential temperature (colored solid contours), cloud water (dashed contours) and rain water (shaded) averaged over 9 grid points at three locations in the southeastern end of the lake (upper panel), the southeastern coast (middle panel) and the Altiplano southeast of the lake. The timeseries start at $t=00$ (25 January 2003 at 7 am Peruvian LST) and end at $t=24$ (26 January 2003 at 7am Peruvian LST).

Skin temperature in °C (shaded) and vertical velocity in m s^{-1} at 600 mb (contour)

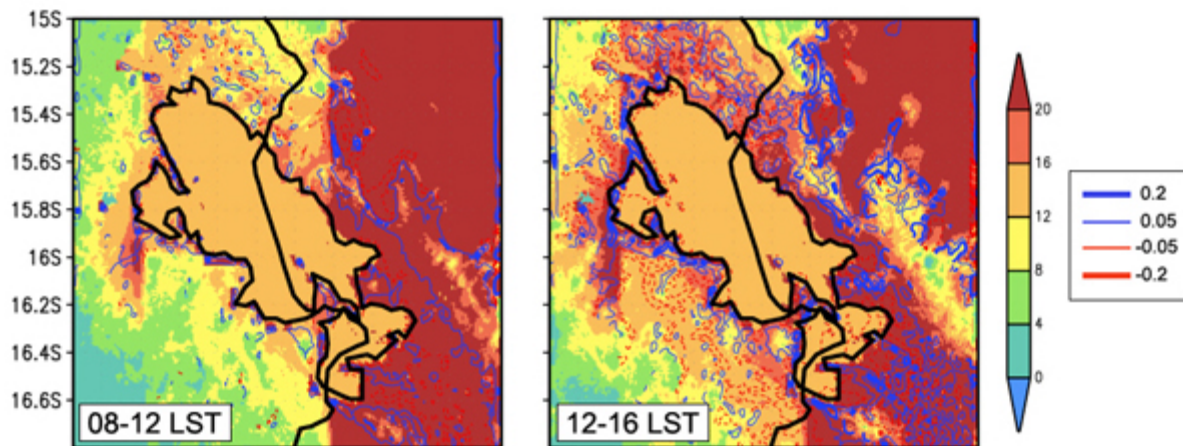


Figure 12. Skin temperature and vertical velocity at 600 mb averaged during 4-hour intervals throughout the 1-km nested simulation.

REFERENCES

Davies-Jones, R., 1993: Useful formulas for computing divergence, vorticity and their errors from three or more stations, *Mon. Wea. Rev.*, 121, 713-172.

Garreaud, R., 1998: Multiscale Analysis of the Summertime Precipitation over the Central Andes, *Monthly Weather Review*, Vol 127, N°5, pp. 901-921.

_____, 2000: Intraseasonal variability of moisture and rainfall over the South American Altiplano, *Monthly Weather Review*, Vol 14, pp. 2779-2789.

_____, and P. Aceituno, 2000: Interannual Variability over the South American Altiplano, *The Journal of Climate*, Vol 14, pp. 2779-2789.

Lenters, J. D., and K. H. Cook, 1995: Simulation and diagnosis of the regional summertime precipitation climatology of South America. *J. Climate*, 8, 2298–3005